Soil Biology and Biochemistry 196 (2024) 109482

Contents lists available at ScienceDirect

Soil Biology and Biochemistry

journal homepage: www.elsevier.com/locate/soilbio

# Nitrifier controls on soil NO and $N_2O$ emissions in three chaparral ecosystems under contrasting atmospheric N inputs

Alexander H. Krichels [a,b,*], Aral C. Greene [b], Elizah Z. Stephens [b], Sharon Zhao [b], Joshua P. Schimel [d], Emma L. Aronson [e], Erin J. Hanan [c], Peter M. Homyak [b]

[a] USDA Forest Service Rocky Mountain Research Station, Albuquerque, NM, USA
[b] Department of Environmental Sciences, University of California, Riverside, CA, USA
[c] Department of Natural Resources and Environmental Science, University of Nevada, Reno, NV, USA
[d] Department of Ecology, Evolution and Marine Biology, University of California, Santa Barbara, CA, USA
[e] Department of Microbiology and Plant Pathology, University of California, Riverside, CA, USA

ARTICLE INFO

*Keywords:*
Nitrous oxide
Nitric oxide
Ammonia oxidizing archaea
Ammonia oxidizing bacteria
Drylands
N saturation

ABSTRACT

High rates of atmospheric N deposition can increase ecosystem N availability and stimulate N losses from soils via nitric oxide (NO; an air pollutant at high concentrations) and nitrous oxide ($N_2O$; a strong greenhouse gas) emissions as predicted by N saturation theory. However, it remains unclear whether theories developed in mesic ecosystems apply to drylands, where plant N uptake and N availability are often decoupled. NO and $N_2O$ are produced during the oxidation of ammonia (i.e., nitrification) by ammonia-oxidizing archaea (AOA) or ammonia-oxidizing bacteria (AOB). Because AOB may be favored in N-rich environments and may emit more NO and $N_2O$ than AOA, high atmospheric N inputs may favor both NO and $N_2O$ emissions. To assess whether atmospheric N deposition favors AOB- and AOA-derived N emissions, we selectively inhibited AOA and AOB and measured NO and $N_2O$ from soils collected from three dryland sites exposed to relatively low (3.8 kg $ha^{-1}$ = Low N) or high (11.8 kg $ha^{-1}$ = High N-A; 15.6 kg $ha^{-1}$ = High N–B) atmospheric N inputs. We found that while the High N–B deposition site had the lowest AOA:AOB ratio (2.3 ± 0.6), consistent with expectations, this site did not emit the most NO and $N_2O$. Rather, AOA emitted between 21 and 78% of the NO from our sites, with higher AOA-derived NO emissions from relatively coarse-textured soils in the Low N deposition site. In addition to nitrification, other processes also emitted NO and $N_2O$, especially in the High N-A site where non-nitrifier NO and $N_2O$ emissions were ~2–4 × higher than the other sites, and where finer textured soils may favor denitrification. Interactions between soil texture and N availability, rather than shifts in nitrifier communities, likely determine whether atmospheric N deposition is retained in these dryland sites or reemitted to the atmosphere as NO or $N_2O$.

## 1. Introduction

Elevated rates of atmospheric nitrogen (N) deposition can enrich soils with N and lead to adverse ecosystem effects such as soil acidification, nutrient imbalances, shifts in species composition, and increased emission of trace gases like nitric oxide (NO; a regional air pollutant at high concentrations) and nitrous oxide ($N_2O$; a powerful greenhouse gas and destroyer of stratospheric ozone) (Fenn et al., 2006; Ravishankara et al., 2009; Bobbink et al., 2010; Yahdjian et al., 2011; Fowler et al., 2013; Tian et al., 2020; Sha et al., 2021). To help determine when atmospheric N inputs exceed the capacity of an ecosystem to retain N, the concept of N saturation was developed in mesic forests, where the negative impacts of N enrichment on ecosystems were first studied (Aber et al., 1989; Lovett and Goodale, 2011). N saturation theory predicts that as ecosystems become enriched with N, NO and $N_2O$ emissions increase in proportion to the N available in excess (Aber et al., 1989). However, in mesic forests, moist soils keep N biogeochemical cycling coupled to ecosystem N sinks (e.g., plants and soil organic matter; Lovett and Goodale, 2011), whereas in drylands, predominantly dry conditions decouple N cycling from N sinks (Homyak et al., 2014; Osborne et al., 2022a). For example, when rainfall rewets dry soils, both biotic and abiotic processes are well known to favor large gaseous N losses before

* Corresponding author. USDA Forest Service Rocky Mountain Research Station, Albuquerque, NM, USA.
*E-mail address:* alexander.krichels@usda.gov (A.H. Krichels).

https://doi.org/10.1016/j.soilbio.2024.109482
Received 12 February 2024; Received in revised form 15 May 2024; Accepted 24 May 2024
Available online 28 May 2024

ecosystem N sinks activate (Homyak et al., 2014; Osborne et al., 2022b; Krichels et al., 2023), suggesting it remains unclear how N-saturation theory applies to dryland environments. Moreover, N pollution may affect N emissions by altering the relative abundance of microorganisms that produce oxidized forms of N during nitrification: ammonia oxidizing bacteria (AOB) and ammonia oxidizing archaea (AOA) (Prosser et al., 2019). Given that AOB may emit more NO and $N_2O$ during nitrification than AOA (Mushinski et al., 2019), understanding how AOA and AOB respond to excess N availability may help determine whether atmospheric N inputs are sequestered or reemitted as NO and $N_2O$ to the atmosphere.

Ammonia oxidizing bacteria and archaea have distinct nitrification pathways that can affect how much N is emitted from soils to the atmosphere. Specifically, AOA may emit less NO than AOB during the oxidation of hydroxylamine ($NH_2OH$), the second step in the sequential oxidation of ammonia to nitrite ($NO_2^-$) via nitrification (Mushinski et al., 2019). During this step, AOA may require NO as a co-reactant to oxidize $NH_2OH$, while AOB do not, making NO more vulnerable to escape to the atmosphere when AOB nitrify (Kozlowski et al., 2016; Prosser et al., 2019). Moreover, AOB can enzymatically reduce NO to $N_2O$—there is no evidence for a similar NO reduction pathway in AOA—allowing for higher nitrifier-derived $N_2O$ emissions in soils where AOB are more active than AOA (Hink et al., 2017; Prosser et al., 2019). While these mechanisms suggest that the AOB nitrification pathway may be "leakier" by emitting more NO and $N_2O$ compared to AOA, both AOA and AOB can release $NH_2OH$ and $NO_2^-$ into the soil environment (Ermel et al., 2018), which can be enzymatically reduced to NO and $N_2O$ via denitrification, or chemically converted to NO and $N_2O$ via chemodenitrification (Firestone and Davidson, 1989; Zhu-Barker et al., 2015; Heil et al., 2016). Nonetheless, nitrification is an important process regulating N trace gas emissions from many drought-prone ecosystems (Homyak et al., 2014; Krichels et al., 2022), and whether the relatively leakier AOB dominate nitrification may influence how much N is lost from ecosystems.

Soil N enrichment may influence whether AOA or AOB dominates nitrification in dry soils. While both AOA and AOB oxidize $NH_3$ to $NH_2OH$, AOA may have higher affinity for $NH_3$ and higher tolerance to withstand drought stress, allowing them to nitrify in drought-stressed environments and recycle N more efficiently (Martens-Habbena et al., 2009; Delgado-Baquerizo et al., 2016; Prosser et al., 2019). In contrast, in N-rich soils, AOB may have more access to $NH_3$, potentially amplifying N trace gas emissions from the relatively leakier AOB nitrification pathway (Prosser et al., 2019; Mushinski et al., 2020). However, N enrichment can also acidify soils if there is enough water to leach base cations (Falkengren-Grerup, 1989; Püspök et al., 2022), which may favor AOA over AOB (Delgado-Baquerizo et al., 2016). Given the many ways in which N pollution may affect nitrifier communities, it remains unclear whether elevated rates of atmospheric N deposition affects NO and $N_2O$ emissions in dryland ecosystems.

In addition to N pollution, drying–rewetting cycles can influence how much NO and $N_2O$ is emitted from drylands. While desiccation can limit soil microbial activity (Moyano et al., 2013), rewetting dry soils can increase soil N availability and stimulate microbial processes that emit NO and $N_2O$ into the atmosphere (Birch, 1958; Homyak et al., 2016; Leitner et al., 2017; Krichels et al., 2022). However, it is not clear whether differences between AOA and AOB nitrification affect rates of N gas efflux during these rewetting events; the contribution of AOA versus AOB to N trace gas emissions has primarily been tested in mesic forested and agricultural ecosystems where soils are relatively moist (Taylor et al., 2013; Thion and Prosser, 2014; Hink et al., 2018; Prosser et al., 2019; Mushinski et al., 2020). Given that dryland ecosystems experience frequent drying-rewetting cycles, with some exposed to among the highest rates of atmospheric N deposition in the world (Fenn et al., 2006; Sickman et al., 2019), we ask: can tradeoffs in AOB and AOA community composition in dryland soils exposed to high rates of atmospheric N deposition affect soil NO and $N_2O$ emissions?

We tested two hypotheses to determine how nitrifier community composition controls N trace gas emissions from dryland ecosystems exposed to elevated N deposition: i) AOB produce more N trace gases than AOA do during rewetting events, and ii) higher soil N availability favors nitrification by AOB compared to AOA, increasing N trace gas emissions from soils exposed to relatively high rates of atmospheric N deposition. To test these hypotheses, we measured soil NO and $N_2O$ emissions from soils collected from three remote chaparral sites exposed to a range of atmospheric N deposition rates in southern California (Table 1). To determine whether AOA or AOB controlled N emissions, we selectively inhibited either AOB nitrification or both AOA and AOB nitrification (Taylor et al., 2013; Mushinski et al., 2019). We also measured the abundance of *amoA* genes (which encode for the first step in nitrification) in AOA and AOB, soil pH, and inorganic N availability at each of the three sites.

## 2. Methods

### 2.1. Study site

We collected soils from three sites exposed to a range of atmospheric N deposition rates in southern California: a Low N deposition site and two high N deposition sites (hereafter, High N-A and High N–B; Table 1; EPA, 2021). Vegetation in all sites was dominated by chamise (*Adenostoma fasciculatum*). Soils from all sites were derived from granite parent material. Soils from the Low N site are fine sandy loams from the Sheephead series and are classified as shallow Entic Haploxerolls. Soils from the High N-A site are coarse loams from the Shepherdsaddle series and are classified as Ultic Haploxeralfs. Finally, soils from the High N–B site are fine sandy loams from the Trigo series and are classified as shallow Typic Xerorthents (Table S1; Soil Survey Staff, Natural Resources Conservation Service, United States Department of Agriculture, 2019). The climate at all sites is Mediterranean with hot, dry summers and cool, wet winters. Annual precipitation ranges from 500 to 670 mm, and average monthly air temperatures range from 8 to 40 °C.

In the year leading up to the experiment, the High N–B deposition site had the highest ambient atmospheric concentrations of $NO_x$ ($NO_x$ = nitric oxide + nitrogen dioxide; 3.60 ± 1.51 ppm), while the High N-A deposition site had the highest ambient atmospheric concentrations of ammonia ($NH_3$; 2.98 ± 2.28 ppm), suggesting that they may receive different forms of N deposition (Fig. S1). The three sites also have slightly different soil textures: the High N-A site is more enriched in clay (38.3 ± 2.57 %) compared to the Low N (20.4 ± 2.92 %) or High N–B sites (15.8 ± 4.93 %; Table 1). Given that soil texture and the form of deposited N varied among the three remote sites, we cannot isolate the effects of N deposition and, instead, aim to: i) understand what controls gaseous N losses from dryland soils and ii) assess how NO and $N_2O$ emissions derived from nitrifiers vary among remote sites that differ in atmospheric N inputs and soil properties.

**Table 1**
Soil physical and chemical properties from the Low N, High N-A, and High N–B deposition sites.

| | pH | Clay (%) | Silt (%) | Latitude | Longitude | Modeled N dep (kg ha$^{-1}$) |
|---|---|---|---|---|---|---|
| Low N | 7.10 ± 0.14 | 20.4 ± 2.92 | 19.6 ± 2.46 | 33.379 | −116.626 | 3.8 |
| High N-A | 6.34 ± 0.31 | 38.3 ± 2.57 | 13.8 ± 1.37 | 36.513 | −118.807 | 11.8 |
| High N–B | 6.17 ± 0.31 | 15.8 ± 4.93 | 8.75 ± 2.09 | 34.203 | −117.794 | 15.6 |

Atmospheric N deposition rates were estimated from the 2019 CMAQ model (EPA, 2021).

### 2.2. Experimental design

At each of the three sites, we collected dry soils (0–10 cm depth; A horizons) from underneath five *Adenostoma fasciculatum* shrubs across a ~50-m transect (each shrub was roughly 10 m apart) in September 2021. We collected soils in September because this is near the end of the dry season at our sites, allowing us to assess the contribution of AOA and AOB to N emissions after experimentally rewetting soils in the lab. Soils were transported back to the lab where they were sieved to 2 mm and stored at 4 °C until the experiment began (soils were refrigerated for less than one month). Soils were removed from the refrigerator two days before beginning the experiment and were incubated at lab temperature (~22 °C). Two soil samples were analyzed at a time. Each soil sample was split into three 50-g subsamples and transferred to canning jars (118 mL volume). The subsamples in each canning jar were exposed to one of three treatments: AOB inhibition, total nitrifier inhibition, or a control (Fig. S7). To inhibit $NH_3$ oxidation by autotrophic AOB, 1-octyne was added to one subsample to bring the headspace in the jar to 4 μmol $L^{-1}$ (Taylor et al., 2013; Mushinski et al., 2019). The 1-octyne was prepared by adding 40 μL of liquid 1-octyne to a 125-mL bottle fitted with a butyl stopper, over-pressurizing the bottle with 100 mL of air, and, once the liquid 1-octyne evaporated, removing 2.7 mL of the bottle headspace to inject into the subsample. To inhibit $NH_3$ oxidation by all autotrophic nitrifiers, acetylene was added to one subsample to bring the jar headspace to 6 μmol $L^{-1}$. The acetylene was prepared by first bubbling acetylene through a sulfuric acid trap to remove impurities, diluting the purified acetylene 10-fold with air, and then injecting 0.28 mL into the subsample. The third jar was treated as a control and was incubated under ambient lab conditions. All jars were incubated for 24 h.

Following the 24-h incubation, NO and $N_2O$ emissions were measured from each jar after experimentally wetting soils. To slow the growth of new AOB after wetting, the jar that was treated with 1-octyene was wet with a solution containing the antibiotic kanamycin at a concentration of 220 μg $g^{-1}$ soil (Mushinski et al., 2019). To slow the growth of any new nitrifying bacteria or archaea, the jar that was treated with acetylene was wetted with a solution containing kanamycin (220 μg $g^{-1}$ soil), the archaeal protein synthesis inhibitor fusidic acid (800 μg $g^{-1}$ soil), and the nitrification inhibitor nitrapyrin (200 μg $g^{-1}$ soil; (Taylor et al., 2013; Mushinski et al., 2019). The control jar was wetted with deionized water only. We note that the addition of bacterial and archaeal growth inhibitors could also limit the growth of non-nitrifying microorganisms that might affect NO and $N_2O$ emissions. However, use of these inhibitors did not significantly affect soil $CO_2$ emissions (Figs. S5 and S6; $p = 0.06$), suggesting their effects on non-nitrifying organisms may be minor during our 46-h incubation. All jars were wetted with enough solution to reach 100% water-holding capacity, designed to simulate rapid rewetting events driving both microbial and abiotic processes and their potential to contribute to N trace gas emissions (Birch, 1958; Austin et al., 2004). NO and $N_2O$ emissions were measured from six of the jars (representing two samples) every 2 h for 46 h after wetting. Net nitrification and net N mineralization rates were measured as the difference in $NO_3^-$ (nitrification) or $NO_3^-$ and $NH_4^+$ (N mineralization) between the start and end of the 46-h incubation. This process was repeated twice weekly until all 45 jars were analyzed (3 sites × 5 replicates × 3 treatments = 45 jars total).

The contribution of AOB to NO and $N_2O$ emissions was determined by subtracting how much NO or $N_2O$ was emitted from the AOB inhibition treatment (i.e., treating soils with 1-octyne and kanamycin) from how much NO or $N_2O$ was emitted from control soils (wetted with water only). The contribution of AOA to NO and $N_2O$ emissions was determined by subtracting how much NO or $N_2O$ was emitted from the total nitrifier inhibition treatment (i.e., treating soils with acetylene, kanamycin, nitrapyrin, and fusidic acid) from how much NO or $N_2O$ was emitted from the AOB inhibition treatment. Finally, NO or $N_2O$ emissions from soils under the total nitrifier inhibition treatment were classified as "other processes", likely including denitrification, heterotrophic nitrification, and/or abiotic reactions. At the low acetylene concentrations used, neither $N_2O$ production from denitrification nor $N_2O$ reduction to $N_2$ should be inhibited (Smith et al., 1978). However, acetylene can oxidize NO to $NO_2^-$ and $NO_3^-$ (Bollmann and Conrad, 1997; Nadeem et al., 2013), potentially lowering N emissions from other processes.

### 2.3. NO and $N_2O$ emissions

Immediately after wetting, six jars (2 samples × 3 treatments) were connected to a recirculating sample loop joining a multiplexer (LI-8150, LI-COR Biosciences), an infrared $CO_2$ gas analyzer (IRGA; LI-8100, LI-COR Biosciences, Lincoln, NE), and an $N_2O$ laser analyzer (Model 914–0027, Los Gatos Research, Inc., Mountain View, CA). To measure $N_2O$ emissions from each jar, air was recirculated through the closed sample loop at a rate of 1.5 L $min^{-1}$. Soil $N_2O$ emissions were calculated as the linear change in $N_2O$ concentrations over a 9-min period. Because the chemiluminescent $NO_2$ analyzer (LMA 3D; Unisearch Associates, Concord, ON, Canada) consumes NO, the $NO_2$ analyzer was not connected to the sample loop during this initial 9-min incubation. Rather, after 9-min, an automated 3-way solenoid valve (Parker Hannifin Corp., Series 11/25/26, #991-000539-006) activated so that the $NO_2$ analyzer pulled from the sample loop at a rate of 1.5 L $min^{-1}$. To replace the air that the $NO_2$ analyzer consumed from each jar (the air from the jars was vented out of the $NO_2$ analyzer into the lab), a second valve activated at the same time to allow zero air (Ultra Grade Zero Air, Airgas, Radnor, PA) to enter each jar at a rate of 1.5 L $min^{-1}$. The $NO_2$ analyzer used a $CrO_3$ converter to oxidize NO to $NO_2$; we did not detect $NO_2$ when $CrO_3$ was removed from the sample loop, suggesting our measurements were mostly NO. NO emissions were calculated using the following equation:

$$\text{NO flux} = \left([\text{NO}]_{\text{outlet}} - [\text{NO}]_{\text{inlet}}\right) \times \text{flow} \times \text{mass N} \div \text{soil wt.} \div \text{R} \div \text{temp} \quad \text{(EQ1)}$$

where $[NO]_{outlet}$ is the concentration of NO leaving the jar headspace (ppb), $[NO]_{inlet}$ is the concentration of NO entering the jar (assumed to be 0 ppb), flow is the flow rate of the sample loop (1.5 L $min^{-1}$), mass N is the molar mass of N in NO (14 g $mol^{-1}$), soil wt. is the mass of soil in the jar (g), R is the molar gas constant (0.0821 L atm $K^{-1}$ $mol^{-1}$), and temp is the room air temperature (Hall et al., 2018). We measured NO concentrations for 10 min while zero air was flowing through the jar, allowing NO concentrations to reach equilibrium within the sample loop. NO fluxes were calculated using the average NO concentrations during the final 30 s of the 10-min incubation. After 10 min, the sample loop was exposed to ambient lab air for 1 min to purge zero air from the sample loop. After this 20-min incubation, the multiplexer connected the next jar to the sample loop, and this process was repeated, allowing us to measure each of the 6 jars once every ~2 h. The continuous stream of dry air decreased soil moisture throughout the 46-h incubation (Fig. S2).

We modified a publicly-available script to calculate $N_2O$ and NO emissions (Andrews and Krichels, 2022). $N_2O$ emissions were calculated as the change in $N_2O$ concentrations over the last 7 min of the incubation when the NO analyzer was not connected to the sample loop. Emissions were considered 0 if the linear relationship between time and $N_2O$ concentrations was not statistically significant ($p > 0.05$). NO emissions were calculated using EQ (1). Both the $N_2O$ and the NO analyzer recorded trace gas concentrations every second. We used the trapezoidal integration (trapZ function in R; Borchers, 2022; R Core Team, 2023) to calculate cumulative $N_2O$ and NO emissions over the 46-h period post-wetting (final units were ng N g dry $soil^{-1}$).

### 2.4. Net nitrification and net N mineralization rates

We measured soil extractable $NO_3^-$ and $NH_4^+$ before wetting soils and

immediately after the 46-h incubation to calculate net nitrification and net N mineralization rates. Briefly, 3 g of soil (dry weight equivalent) were extracted in 30 mL 2M KCl for 1 h, filtered (Whatman 42 filter paper; 2.5 μm pore size), and the extracts were then frozen until analysis. Extracts were analyzed for $NO_3^-$ (SEAL method EPA-126-A) and $NH_4^+$ (SEAL method EPA-129-A) using colorimetric assays in the Environmental Sciences Research Laboratory at UC Riverside (https://envisci.ucr.edu/research/environmental-sciences-research-laboratory-esrl). Net nitrification and net N mineralization rates were calculated as the difference in inorganic N ($NO_3^-$ for nitrification and $NO_3^-$ plus $NH_4^+$ for net N mineralization) before and after the incubation divided by the length of the incubation (~46 h). While nitrifiers may not mineralize N, nitrification can emit N trace gases or supply $NO_3^-$ to denitrifiers, which can affect the calculation of net N mineralization rates. We also measured soil gravimetric water content by drying soil samples (~10 g) at 104 °C for 24 h. We estimated 100% soil water holding capacity (WHC) as the amount of water held by soils after saturating them with water and allowing them to drain in an air-tight container (to limit evaporation) for 8 h.

### 2.5. *amoA* gene quantification

A subsample (~5 g) of each soil sample ($n = 15$) was frozen (−20 °C) as soon as soils arrived in the lab. Within one month of freezing, DNA was extracted from 0.25 g of each subsample using a DNA extraction kit (Qiagen DNeasy PowerSoil Pro, Hilden, Germany) following the manufacturer's guidelines after an overnight incubation to enhance DNA extraction (700 μL CD1 + 100 μL ATL at 4 °C; Qiagen). Quantitative polymerase chain reaction (qPCR) was used to estimate the abundance of bacterial and archaeal *amoA* genes (Beman et al., 2008); the AmoA1F/amoA2R primer set was used for bacteria (Rotthauwe et al., 1997) and the Arch-amoAF/ArchamoAR primer set was used for archaea (Francis et al., 2005). Each qPCR was run in 10 μL reactions containing 5 μL master mix (Forget-Me-Not EvaGreen qPCR Master Mix, Biotium, Inc., Fremont, CA), 0.8 μL of 2 mM $MgCl_2$, 0.25 μL of 0.5 mg $mL^{-1}$ bovine serum albumin, 0.125 μL of 0.25 μM forward and reverse primer, 2.5 μL $H_2O$, and 1.2 μL sample DNA. Bacterial *amoA* was amplified using the following protocol: 5 min at 95 °C, followed by 40 cycles of 45 s at 95 °C, 30 s at 56 °C and 60 s at 72 °C (CFX384 Touch Real-Time PCR Detection System, Bio-Rad, Hercules, CA). Archaeal *amoA* was amplified using the following protocol: 4 min at 95 °C, followed by 40 cycles of 30 s at 95 °C, 45 s at 53 °C and 60 s at 72 °C. The standard sequences were chosen from well-known archaeal (crenarchaeota genomic fragment 54d9) and bacterial (*amo*A gene of *Nitrosomonas europaea* ATCC, 19718) ammonia oxidizing microorganisms. Standard curves were prepared using serial dilutions for bacterial *amoA* ($10^6$ to $10^2$ copies) and archaeal *amoA* ($10^7$ to $10^3$ copies). The bacterial *amoA* standards had efficiencies of 83.5% ($R^2 = 0.998$) and archaeal *amoA* standards had efficiencies of 66.9% ($R^2 = 0.997$).

### 2.6. Atmospheric N deposition

We used the Community Multiscale Air Quality Modeling System (CMAQ) to estimate total N deposition rates at our three sites. We report data from measurement-model "fused" outputs that estimate total N deposition rates in 2019 (the most recent year from which modeled N deposition data were available) (EPA, 2021).

We also used passive atmospheric samplers to estimate the relative contribution of reduced N (ammonia; $NH_3$) and oxidized N ($NO + NO_2$; $NO_x$) to atmospheric N deposition at each site. Passive samplers (Ogawa pads; Ogawa USA, Pompano Beach, FL) chemically pretreated to absorb $NO_x$ or $NH_3$ were installed ~1 m above the ground at each site (two samplers per site). The passive samplers were left in the field for approximately one month during the spring, winter, summer, and fall seasons (i.e., four one-month periods), followed by analysis for N content at the USDA Forest Service fire laboratory in Riverside, CA. Atmospheric ambient $NO_x$ and $NH_3$ concentrations were then estimated according to manufacturer instructions (https://ogawausa.com/), from which we calculated the one-year average concentration for each species using the four seasonal measurements. While we did not estimate N deposition rates, atmospheric $NO_x$ and $NH_3$ concentrations were used to compare which N species dominated N deposition at our three sites.

### 2.7. Statistical analyses

All statistics were conducted in R version 4.3.1 (R Core Team, 2023). We used two-way analysis of variance (ANOVA) to assess if cumulative NO emissions, cumulative $N_2O$ emissions, or net N transformation rates differed between sites and in response to experimental treatments (i.e., selectively inhibiting AOB nitrification and total nitrification). Similarly, we used one-way ANOVA to assess if AOA abundance, AOB abundance, or initial soil N concentrations differed among sites. If the one-way ANOVA was significant ($p < 0.05$), we used Tukey-corrected multiple comparisons to assess which sites differed from one another. Model residuals were assessed for normality using the olsrr package in R (Hebbali, 2020) and log transformations were applied when residuals did not follow a normal distribution; this was only the case for *amoA* gene abundance from AOB.

## 3. Results

### 3.1. NO and $N_2O$ emissions

Wetting dry soils without nitrification inhibitors increased NO emissions at our three sites, averaging 136 ± 21.5 ng N–NO $g^{-1}$ (hereafter, ±standard error), but the emissions did not significantly differ among the sites (Fig. 1A; $F_{2,36} = 0.22$, $p = 0.80$). Adding nitrification inhibitors to soils produced a significant treatment effect ($F_{2,36} = 4.86$, $p = 0.014$), with this effect driven by the 26–72% reduction in NO emissions when both AOA and AOB nitrification were inhibited by acetylene (Fig. 1A). In contrast to using acetylene, treating soils with 1-octyne to exclusively inhibit AOB nitrification never altered NO emissions by more than 10% compared to control soils (Fig. 1A).

While soil $N_2O$ emissions were of similar magnitude and variability to NO, they were higher in the High N-A deposition site (463 ± 188 ng $N–N_2O$ $g^{-1}$ from control soils without inhibitors) than in either the Low (124 ± 70.6 ng $N–N_2O$ $g^{-1}$) or High N–B deposition sites (182 ± 90.5 ng $N–N_2O$ $g^{-1}$; $F_{2,36} = 10.5$, $p < 0.001$; Fig. 2). In contrast to NO emissions, using nitrification inhibitors did not affect $N_2O$ emissions, either 1-octyne to inhibit AOB nitrification or acetylene to inhibit both AOA and AOB nitrification ($F_{2,36} = 0.15$, $p = 0.76$).

### 3.2. Soil inorganic N and net N transformation rates

Soils exposed to elevated N deposition rates had generally higher extractable $NH_4^+$ concentrations. $NH_4^+$ concentrations in dry soils prior to lab incubations were 1.5 × higher in the High N-A deposition site (3.32 ± 0.23 μg $NH_4^+$-N $g^{-1}$) than in the Low N deposition site (2.15 ± 0.26 μg $NH_4^+$-N $g^{-1}$; Fig. 3A), but the difference was only significant at $p = 0.07$. In contrast, $NH_4^+$ did not differ between the High N-A and High N–B deposition site (2.68 ± 0.47 μg $NH_4^+$-N $g^{-1}$; $p = 0.39$). Soil $NO_3^-$ followed similar patterns to soil $NH_4^+$. Soil $NO_3^-$ in dry soils differed among sites ($F_{2,12} = 5.7$, $p = 0.02$); $NO_3^-$ was higher in the High N-A (1.52 ± 0.48 μg $NO_3^-$-N $g^{-1}$) than in both the Low (0.20 ± 0.11 μg $NO_3^-$-N $g^{-1}$; $p = 0.02$) and High N–B deposition sites (0.40 ± 0.15 μg $NO_3^-$-N $g^{-1}$; $p = 0.05$; Fig. 3B), but $NO_3^-$ did not differ between the Low and High N–B deposition sites ($p = 0.88$).

Consistent with having the highest soil $NH_4^+$ and $NO_3^-$ concentrations, Net N mineralization rates were highest in the High N-A deposition site (0.60 ± 0.082 μ g N $g^{-1}$ $hr^{-1}$ in control soils without nitrification inhibitors; Fig. 4A) and responded differently to inhibitor treatments in each site (treatment by site interaction $F_{4,34} = 2.73$, $p =$

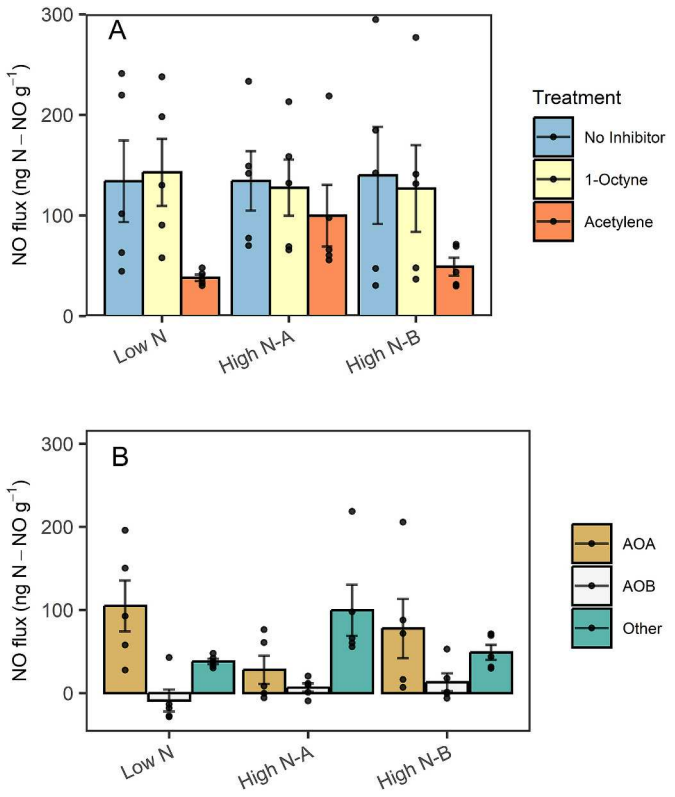


**Fig. 1.** Cumulative NO emissions (ng N–NO $g^{-1}$ dry soil) over the course of incubating soils for ~48 h after wetting. The top panel (A) shows NO emissions after treating soils with only water, 1-octyne (AOB inhibitor), or acetylene (AOA and AOB inhibitor). The bottom panel (B) shows the contribution of AOA, AOB, and heterotrophs to NO emissions. AOB-derived NO emissions were determined by subtracting how much NO was emitted from the AOB inhibition treatment from how much NO was emitted from the control. AOA-derived NO emissions were determined by subtracting how much NO was emitted from the total nitrifier inhibition treatment from how much NO was emitted from the AOB inhibition treatment. Finally, heterotrophic NO emissions were assumed equal to the NO emitted under acetylene. Bars represent the mean, error bars represent one standard error of the mean, and dots represent individual observations (n = 5).

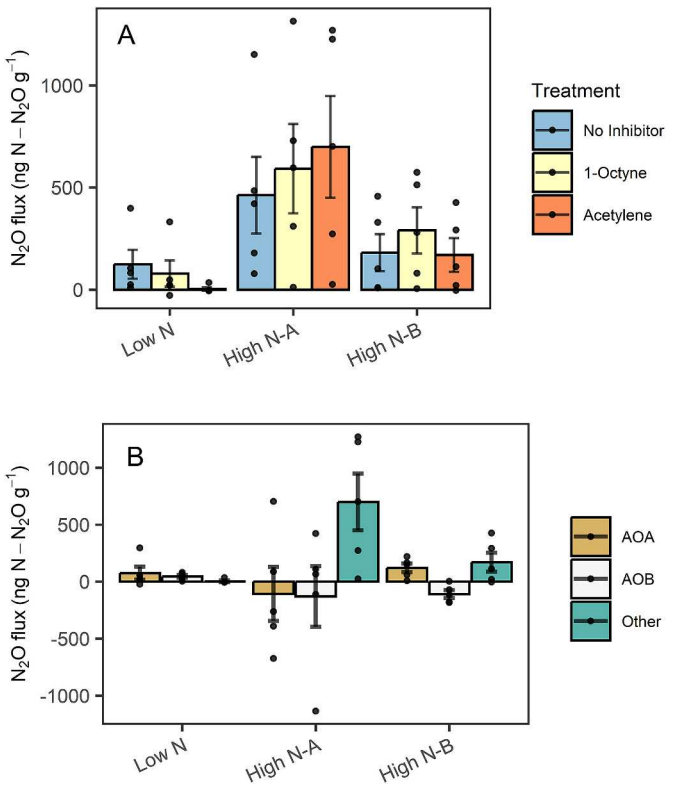


**Fig. 2.** Cumulative $N_2O$ emissions (ng N–$N_2O$ $g^{-1}$ dry soil) over the course of incubating soils for ~48 h after wetting. The top panel (A) shows $N_2O$ emissions after treating soils with only water, (AOB inhibitor), or acetylene (AOA and AOB inhibitor). The bottom panel (B) shows the contribution of AOA, AOB, and heterotrophs to NO emissions. AOB-derived $N_2O$ emissions were determined by subtracting how much $N_2O$ was emitted from the AOB inhibition treatment from how much $N_2O$ was emitted from control soils. AOA-derived $N_2O$ emissions were determined by subtracting how much $N_2O$ was emitted from the total nitrifier inhibition treatment from how much $N_2O$ was emitted from the AOB inhibition treatment. Finally, heterotrophic $N_2O$ emissions were assumed equal to the $N_2O$ emitted under acetylene. Bars represent the mean, error bars represent one standard error of the mean, and dots represent individual observations (n = 5).

0.045). Inhibiting AOB nitrification with 1-octyne decreased net N mineralization rates by 24% in soils from the High N-A deposition site (Fig. 4A). Net N mineralization rates were lower in the High N–B deposition site (0.12 ± 0.027 μ g N $g^{-1}$ $hr^{-1}$ in control soils) and decreased by 102% when AOA and AOB nitrification was inhibited with acetylene. Net N mineralization rates in soils from the Low N deposition site were close to zero in all treatments.

Net nitrification rates were highest in the Low N deposition site relative to other sites (0.081 ± 0.022 μ g N $g^{-1}$ $hr^{-1}$ in control soils; $F_{2,34} = 11.7$, $p < 0.001$; Fig. 4B) and did not consistently respond to the inhibition treatments at any of the sites ($F_{2,34} = 0.62$, p = 0.54). The lack of treatment effect likely stems from variable rates that were all close to zero in soils from the High N-A and High N–B deposition sites (Fig. 4B). In the Low N deposition site, inhibiting AOB nitrification with 1-octyne did not decrease nitrification rates, while inhibiting AOA and AOB nitrification with acetylene decreased nitrification rates by 66%.

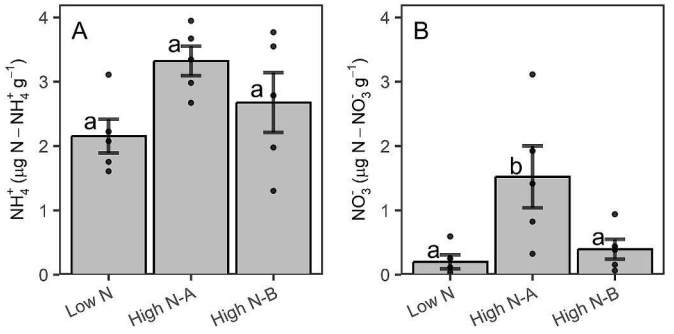


**Fig. 3.** (A) Soil extractable $NH_4^+$ and (B) $NO_3^-$ concentrations in dry soils from our three sites. Bars represent the mean, error bars represent one standard error of the mean, and dots represent individual observations (n = 5). Lower case letters represent statistical significance (p < 0.05).

### 3.3. AOA and AOB amoA gene abundance

*amoA* gene abundance from AOA was higher in both the High N-A ($1.48 \times 10^6 \pm 3.20 \times 10^5$ gene copies $g^{-1}$) and Low N deposition sites ($1.27 \times 10^6 \pm 1.93 \times 10^5$ gene copies $g^{-1}$) than in the High N–B deposition site ($6.27 \times 10^5 \pm 2.35 \times 10^5$ gene copies $g^{-1}$; Fig. 5A), but this was only significant at p = 0.085 ($F_{2,12} = 3.05$). In contrast, *amoA* gene abundance from AOB did not differ among sites ($F_{2,12} = 1.27$, $p = 0.316$), averaging $2.3 \times 10^5 \pm 2.1 \times 10^4$ gene copies $g^{-1}$ across all sites (Fig. 5B). The ratio of *amoA* genes in AOA relative to AOB was highest in the Low N deposition site (7.07 ± 1.25) and lowest in the High N–B deposition site (2.33 ± 0.57; $F_{2,12} = 6.00$, $p = 0.016$; Fig. 5C).

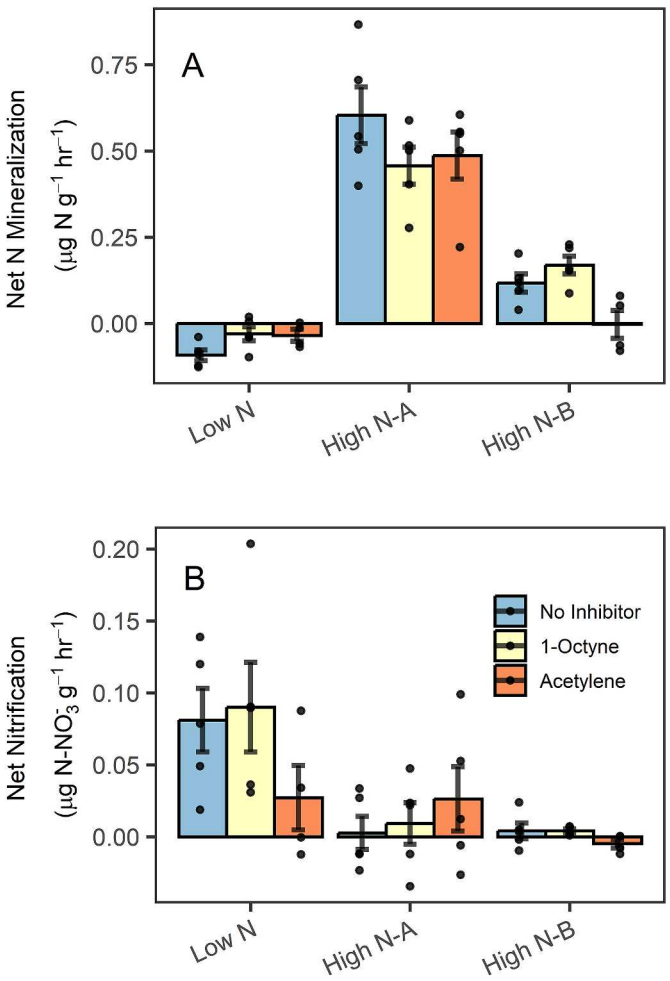


**Fig. 4.** Net rates of (A) N mineralization and (B) nitrification over the ~48-h incubations after wetting soils with water, 1-Octyne (AOB inhibitor), or Acetylene (AOA and AOB inhibitor). Bars represent the mean, error bars represent one standard error of the mean, and dots represent individual observations (n = 5).

## 4. Discussion

N saturation theory predicts that as N inputs exceed the capacity of ecosystems to assimilate N, N losses via gaseous pathways will increase in proportion to the N available in excess (Aber et al., 1989; Lovett and Goodale, 2011; Homyak et al., 2014). Here, we studied whether high rates of atmospheric N inputs can increase gaseous N losses by lowering the AOA:AOB ratio of nitrifiers, potentially altering nitrifier efficiency and, thereby, amplifying soil N trace gas emissions from drylands (Liu et al., 2017; Mushinski et al., 2019; Prosser et al., 2019). Our measurements suggest that while higher atmospheric N deposition rates are consistent with relatively low AOA:AOB ratios as hypothesized, this change in nitrifier community composition did not correspond with differences in NO and $N_2O$ emissions among sites. Furthermore, NO emissions were primarily derived from AOA, even at the sites with the highest N inputs, in contrast to the hypothesis that AOB would dominate NO production with increasing atmospheric N inputs. While N deposition was not associated with higher nitrifier-derived NO emissions, the site exposed to the highest atmospheric concentrations of reduced N species (i.e., $NH_3$) had both the highest soil N concentrations and NO and $N_2O$ emissions from non-nitrifying processes, consistent with predictions based on N saturation theory and with the assessment that this site may be N saturated (Michalski et al., 2004).

High rates of atmospheric N deposition were associated with low AOA:AOB ratios, consistent with the expectation that higher soil N availability would favor AOB over AOA (Thion and Prosser, 2014; Delgado-Baquerizo et al., 2016; Prosser et al., 2019; Mushinski et al., 2020). However, the relative abundance of AOA versus AOB nitrifiers did not explain differences in NO emissions among sites. In fact, AOB abundance and AOB-derived NO emissions were consistently low in all three sites (Fig. 1B; Fig. 5)—regardless of soil N availability (Fig. 3)—suggesting that chronic N enrichment does not always favor increased AOB-derived NO emissions in these drylands. Perhaps there were not enough AOB in these dry soils to produce appreciable amounts of NO, consistent with the fewer AOB we observed relative to temperate forests (Mushinski et al., 2019) and mesic agricultural systems (Hink et al., 2017), both of which found that AOB emitted more N than AOA. Thus, despite relatively high rates of atmospheric N deposition, relatively small AOB populations in our dryland sites may limit AOB-derived N trace gas emissions and their predictive power for estimating N losses via NO.

In contrast to AOB nitrification, AOA nitrification emitted between 21 and 78% of the total NO from all three sites (Fig. 1). Even though AOA were much more abundant than AOB in our sites (Fig. 5), it is still surprising AOA controlled NO emissions post-wetting, as they are not often associated with substantial NO production during nitrification (Mushinski et al., 2019). In these dryland sites, it is possible that AOA nitrification released nitrification intermediates ($NO_2^-$ and/or $NH_2OH$) into the soil environment, producing NO via chemodenitrification or denitrification (Zhu-Barker et al., 2015; Heil et al., 2016). We also found that while NO emissions were similar from all three sites during lab incubations, NO production by AOA varied independent of atmospheric N deposition rates. AOA-derived NO emissions and AOA net nitrification rates were highest in the Low N deposition site, consistent with the hypothesis that AOA outcompete AOB in low-N environments. However, AOA-derived NO emissions were also elevated in the High N–B deposition site, where AOA abundance was low, suggesting that other factors

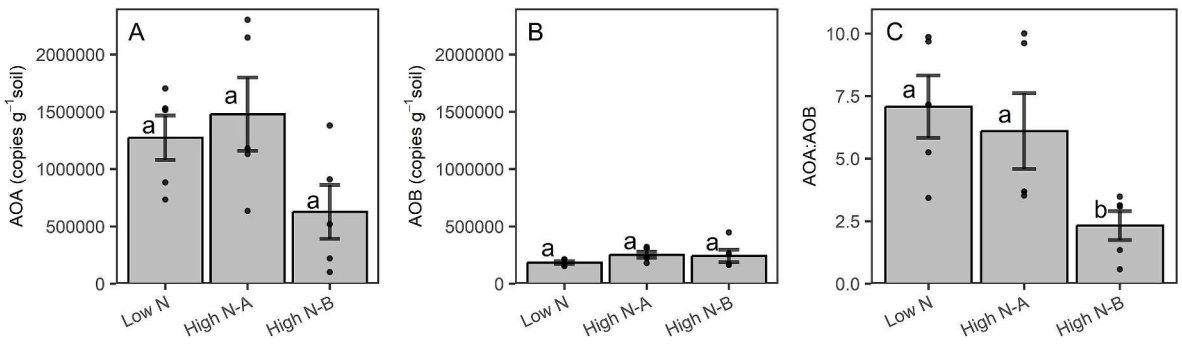


**Fig. 5.** Abundance of the *amoA* gene in (A) ammonia oxidizing archaea (AOA), (B) ammonia oxidizing bacteria (AOB), and (C) the ratio of *amoA* genes in AOA relative to AOB. Bars represent the mean, error bars represent one standard error of the mean, and dots represent individual observations (n = 5). Lower case letters represent statistical significance ($p < 0.05$).

in addition to N availability and AOA abundance determine how much NO is produced by AOA. For example, coarse-textured soils in the Low and High N–B deposition sites held less water throughout the lab incubation (Table 1; Fig. S2), suggesting that faster drying could have increased oxygen diffusion, allowing nitrification—an aerobic process—to emit more NO regardless of soil N availability. Conversely, finer soil texture in the High N-A deposition site drained water more slowly during the lab incubation (Fig. S2), potentially slowing oxygen diffusion (Lacroix et al., 2023) and, thereby, hindering nitrifier-derived NO emissions despite high AOA abundance. Such dynamics are consistent with studies that demonstrate soil edaphic properties, not only N availability and nitrifier communities, control N cycling in dryland ecosystems (Scholes et al., 1997; Osborne et al., 2022b; Ren et al., 2024).

Beyond the contribution of AOA and AOB to NO and $N_2O$ emissions, other processes, such as heterotrophic nitrification, abiotic reactions, and/or denitrification, produced over 20% of the NO emitted from the Low and High N–B deposition sites, and roughly 74% of NO emitted from the High N-A deposition site. Of these processes, heterotrophic nitrification likely contributed the least given the $NH_4^+$-poor soils at our study sites that limit this process (Song et al., 2021). In the slightly more acidic soils found in the High N–B and High N-A deposition sites, it is possible lower pH may have promoted abiotic decomposition of nitrite to NO (Slessarev et al., 2021) or hydroxylamine to $N_2O$ (Zhu-Barker et al., 2015). In addition to abiotic processes, the high $NO_3^-$ concentrations in the High N-A site may have also stimulated denitrification, especially given the higher clay content in these soils that could have limited $O_2$ diffusion and favored anaerobic conditions at 100% WHC required for denitrification (Sexstone et al., 1985; Lacroix et al., 2023). In support of a dominant role by denitrification, the High N-A deposition site emitted the most $N_2O$, exceeding NO emission rates, and suggesting $N_2O$ can potentially dominate gaseous N losses from drylands relative to NO (Eberwein et al., 2020; Krichels et al., 2022). We also note that the High N-A deposition site is exposed to more atmospheric $NH_3$ than $NO_x$, likely due to its proximity to agricultural land in the San Joaquin Valley (Li et al., 2016), and that we also measured the highest net N mineralization rates at this site (Fig. 4A). Because retention of $NH_4^+$ in clays is greater than for oxidized forms of N (Johnston and Tombácz, 2002), drylands exposed to $NH_3$ deposition may be more at risk of becoming saturated with N and favor $N_2O$ emissions via denitrification and/or abiotic reactions when soils saturate with water during the wet season.

## 5. Conclusions

We found that the dryland soils exposed to high rates of atmospheric N deposition did not always emit more NO and $N_2O$ to the atmosphere than soils from the low N deposition site, as N saturation theory would predict. While high rates of atmospheric N deposition were associated with lower soil AOA:AOB ratios, the relative abundance of AOA versus AOB did not predict N trace gas emissions, suggesting it is not a robust indicator of N saturation status. Rather, AOA-derived NO emissions were favored in coarse-textured soils, suggesting that edaphic variables must be considered when forecasting soil N dynamics as ecosystems saturate with N. Nevertheless, soil inorganic N was elevated in the site exposed to the highest concentrations of atmospheric $NH_3$ relative to $NO_x$ (but not the site with the highest rates of total N deposition), corresponding to higher NO and $N_2O$ emissions from denitrification and/or abiotic reactions. Interactions between soil texture, atmospheric deposition of $NH_3$ vs. $NO_x$, and soil N availability may, therefore, determine whether atmospheric N deposition is retained in dryland ecosystems or emitted as NO (an air pollutant at high concentrations) and $N_2O$ (a strong greenhouse gas).

## CRediT authorship contribution statement

**Alexander H. Krichels:** Writing – review & editing, Writing – original draft, Visualization, Validation, Supervision, Project administration, Methodology, Investigation, Formal analysis, Data curation, Conceptualization. **Aral C. Greene:** Writing – review & editing, Investigation, Data curation, Conceptualization. **Elizah Z. Stephens:** Writing – review & editing, Methodology, Data curation, Conceptualization. **Sharon Zhao:** Writing – review & editing, Investigation, Data curation. **Joshua P. Schimel:** Writing – review & editing, Supervision, Funding acquisition, Conceptualization. **Emma L. Aronson:** Writing – review & editing, Resources, Methodology, Funding acquisition, Conceptualization. **Erin J. Hanan:** Writing – review & editing, Project administration, Funding acquisition, Conceptualization. **Peter M. Homyak:** Writing – review & editing, Writing – original draft, Validation, Supervision, Resources, Project administration, Methodology, Investigation, Funding acquisition, Conceptualization.

## Declaration of competing interest

The authors declare the following financial interests/personal relationships which may be considered as potential competing interests:

Dr. Schimel serves on the editorial board for Soil Biology and Biochemistry but was not involved in handling this manusctipt. If there are other authors, they declare that they have no known competing financial interests or personal relationships that could have appeared to influence the work reported in this paper.

## Data availability

All data are publically available in the Dryad data repository: https://doi.org/10.5061/dryad.xpnvx0kp0.

## Acknowledgements

We thank Johann Püspök and Tony Calma for their help collecting soils. We also thank Beatriz Vindiola, David Jones, and David Lyons for their help analyzing samples in the lab. This work was funded by the National Science Foundation (DEB 1916622) and supported in part by the USDA Forest Service Rocky Mountain Research Station. The findings and conclusions in this publication are those of the authors and should not be construed to represent any official USDA or U.S. Government determination or policy.

## Appendix A. Supplementary data

Supplementary data to this article can be found online at https://doi.org/10.1016/j.soilbio.2024.109482.

## References

Aber, J.D., Nadelhoffer, K.J., Steudler, P., Melillo, J.M., 1989. Nitrogen saturation in northern forest ecosystems. BioScience 39, 378–386.
Andrews, H.M., Krichels, A.H., 2022. Handr003/TraceGasArray: v1.1 (v1.1). Zenodo. https://doi.org/10.5281/zenodo.7246428.
Austin, A.T., Yahdjian, L., Stark, J.M., Belnap, J., Porporato, A., Norton, U., Ravetta, D. A., Schaeffer, S.M., 2004. Water pulses and biogeochemical cycles in arid and semiarid ecosystems. Oecologia 141, 221–235.
Beman, J.M., Popp, B.N., Francis, C.A., 2008. Molecular and biogeochemical evidence for ammonia oxidation by marine Crenarchaeota in the Gulf of California. The ISME Journal 2, 429–441.
Birch, H.F., 1958. The effect of soil drying on humus decomposition and nitrogen availability. Plant and Soil 10, 9–31.
Bobbink, R., Hicks, K., Galloway, J., Spranger, T., Alkemade, R., Ashmore, M., Bustamante, M., Cinderby, S., Davidson, E., Dentener, F., Emmett, B., Erisman, J.-W., Fenn, M., Gilliam, F., Nordin, A., Pardo, L., De Vries, W., 2010. Global assessment of nitrogen deposition effects on terrestrial plant diversity: a synthesis. Ecological Applications: A Publication of the Ecological Society of America 20, 30–59.
Bollmann, A., Conrad, R., 1997. Acetylene blockage technique leads to underestimation of denitrification rates in oxic soils due to scavenging of intermediate nitric oxide. Soil Biology and Biochemistry 29, 1067–1077.
Borchers, H., 2022. Pracma: Practical Numerical Math Functions.
Delgado-Baquerizo, M., Maestre, F.T., Eldridge, D.J., Singh, B.K., 2016. Microsite differentiation drives the abundance of soil ammonia oxidizing bacteria along aridity gradients. Frontiers in Microbiology 7, 1–11.

Eberwein, J.R., Homyak, P.M., Carey, C.J., Aronson, E.L., Jenerette, G.D., 2020. Large nitrogen oxide emission pulses from desert soils and associated microbiomes. Biogeochemistry 149, 239–250.

Epa, U.S., 2021. EQUATESv1.0: Emissions, WRF/MCIP, CMAQv5.3.2 Data – 2002-2019 US_12km and NHEMI_108km. https://doi.org/10.15139/S3/F2KJSK.

Ermel, M., Behrendt, T., Oswald, R., Derstroff, B., Wu, D., Hohlmann, S., Stönner, C., Pommerening-Röser, A., Könneke, M., Williams, J., Meixner, F.X., Andreae, M.O., Trebs, I., Sörgel, M., 2018. Hydroxylamine released by nitrifying microorganisms is a precursor for HONO emission from drying soils. Scientific Reports 8, 1–8.

Falkengren-Grerup, U., 1989. Soil acidification and its impact on ground vegetation. Ambio 18, 179–183.

Fenn, M., Baron, J.S., Allen, E.B., Rueth, H.M., Nydick, K.R., Geiser, L., Bowman, W.D., Sickman, J.O., Meixner, T., Johnson, D.W., Neitlich, P., 2006. Ecological effects of nitrogen deposition in the western United States. BioScience 53, 404.

Firestone, M.K., Davidson, E.A., 1989. Microbiological basis of NO and $N_2O$ production and consumption in soil. In: Exchange of Trace Gases between Terrestrial Ecosystems and the Atmosphere, pp. 7–21.

Fowler, D., Coyle, M., Skiba, U., Sutton, M.A., Cape, J.N., Reis, S., Sheppard, L.J., Jenkins, A., Grizzetti, B., Galloway, J.N., Vitousek, P., Leach, A., Bouwman, A.F., Butterbach-Bahl, K., Dentener, F., Stevenson, D., Amann, M., Voss, M., 2013. The global nitrogen cycle in the Twentyfirst century. Philosophical Transactions of the Royal Society of London. Series B, Biological Sciences 368. https://doi.org/10.1098/rstb.2013.0164.

Francis, C.A., Roberts, K.J., Beman, J.M., Santoro, A.E., Oakley, B.B., 2005. Ubiquity and diversity of ammonia-oxidizing archaea in water columns and sediments of the ocean. Proceedings of the National Academy of Sciences of the United States of America 102, 14683–14688.

Hall, S.J., Reyes, L., Huang, W., Homyak, P.M., 2018. Wet Spots as Hotspots: moisture responses of nitric and nitrous oxide emissions from poorly drained agricultural soils. Journal of Geophysical Research: Biogeosciences 123, 3589–3602.

Hebbali, A., 2020. Olsrr: Tools for Building OLS Regression Models.

Heil, J., Vereecken, H., Brüggemann, N., 2016. A review of chemical reactions of nitrification intermediates and their role in nitrogen cycling and nitrogen trace gas formation in soil. European Journal of Soil Science 67, 23–39.

Hink, L., Gubry-Rangin, C., Nicol, G.W., Prosser, J.I., 2018. The consequences of niche and physiological differentiation of archaeal and bacterial ammonia oxidisers for nitrous oxide emissions. The ISME Journal 12, 1084–1093.

Hink, L., Nicol, G.W., Prosser, J.I., 2017. Archaea produce lower yields of $N_2O$ than bacteria during aerobic ammonia oxidation in soil. Environmental Microbiology 19, 4829–4837.

Homyak, P.M., Blankinship, J.C., Marchus, K., Lucero, D.M., Sickman, J.O., Schimel, J.P., 2016. Aridity and Plant Uptake Interact to Make Dryland Soils Hotspots for Nitric Oxide (NO) Emissions, vol. 113. Proceedings of the National Academy of Sciences, pp. E2608–E2616.

Homyak, P.M., Sickman, J.O., Miller, A.E., Melack, J.M., Meixner, T., Schimel, J.P., 2014. Assessing nitrogen-saturation in a seasonally dry chaparral watershed: limitations of traditional indicators of N-Saturation. Ecosystems 17, 1286–1305.

Johnston, C.T., Tombácz, E., 2002. Surface chemistry of soil minerals. In: Soil Mineralogy with Environmental Applications. Soil Science Society of America, Madison, WI, USA, pp. 37–67.

Kozlowski, J.A., Stieglmeier, M., Schleper, C., Klotz, M.G., Stein, L.Y., 2016. Pathways and key intermediates required for obligate aerobic ammonia-dependent chemolithotrophy in bacteria and Thaumarchaeota. The ISME Journal 10, 1836–1845.

Krichels, A.H., Homyak, P.M., Aronson, E.L., Sickman, J.O., Botthoff, J., Shulman, H., Piper, S., Andrews, H.M., Jenerette, G.D., 2022. Rapid nitrate reduction produces pulsed NO and $N_2O$ emissions following wetting of dryland soils. Biogeochemistry 158, 233–250.

Krichels, A.H., Jenerette, G.D., Shulman, H., Piper, S., Greene, A.C., Andrews, H.M., Botthoff, J., Sickman, J.O., Aronson, E.L., Homyak, P.M., 2023. Bacterial denitrification drives elevated $N_2O$ emissions in arid southern California drylands. Science Advances 9, eadj1989.

Lacroix, E.M., Aeppli, M., Boye, K., Brodie, E., Fendorf, S., Keiluweit, M., Naughton, H.R., Noël, V., Sihi, D., 2023. Consider the anoxic microsite: acknowledging and appreciating spatiotemporal redox heterogeneity in soils and sediments. ACS Earth and Space Chemistry. https://doi.org/10.1021/acsearthspacechem.3c00032.

Leitner, S., Homyak, P.M., Blankinship, J.C., Eberwein, J., Jenerette, G.D., Zechmeister-Boltenstern, S., Schimel, J.P., 2017. Linking NO and $N_2O$ emission pulses with the mobilization of mineral and organic N upon rewetting dry soils. Soil Biology and Biochemistry 115, 461–466.

Li, Y., Schichtel, B.A., Walker, J.T., Schwede, D.B., Chen, X., Lehmann, C.M.B., Puchalski, M.A., Gay, D.A., Collett Jr., J.L., 2016. Increasing importance of deposition of reduced nitrogen in the United States. Proceedings of the National Academy of Sciences of the United States of America 113, 5874–5879.

Liu, S., Han, P., Hink, L., Prosser, J.I., Wagner, M., Brüggemann, N., 2017. Abiotic conversion of extracellular $NH_2OH$ contributes to $N_2O$ emission during ammonia oxidation. Environmental Science and Technology 51, 13122–13132.

Lovett, G.M., Goodale, C.L., 2011. A new conceptual model of nitrogen saturation based on experimental nitrogen addition to an oak forest. Ecosystems 14, 615–631.

Martens-Habbena, W., Berube, P.M., Urakawa, H., de la Torre, J.R., Stahl, D.A., 2009. Ammonia oxidation kinetics determine niche separation of nitrifying Archaea and Bacteria. Nature 461, 976–979.

Michalski, G., Meixner, T., Fenn, M., Hernandez, L., Sirulnik, A., Allen, E., Thiemens, M., 2004. Tracing atmospheric nitrate deposition in a complex semiarid ecosystem using delta17O. Environmental Science and Technology 38, 2175–2181.

Moyano, F.E., Manzoni, S., Chenu, C., 2013. Responses of soil heterotrophic respiration to moisture availability: an exploration of processes and models. Soil Biology and Biochemistry 59, 72–85.

Mushinski, R.M., Payne, Z.C., Raff, J.D., Craig, M.E., Pusede, S.E., Rusch, D.B., White, J. R., Phillips, R.P., 2020. Nitrogen Cycling Microbiomes Are Structured by Plant Mycorrhizal Associations with Consequences for Nitrogen Oxide Fluxes in Forests, pp. 1–15.

Mushinski, R.M., Phillips, R.P., Payne, Z.C., Abney, R.B., Jo, I., Fei, S., 2019. Microbial Mechanisms and Ecosystem Flux Estimation for Aerobic $NO_y$ Emissions from Deciduous Forest Soils. https://doi.org/10.1073/pnas.1814632116.

Nadeem, S., Dörsch, P., Bakken, L.R., 2013. Autoxidation and acetylene-accelerated oxidation of NO in a 2-phase system: implications for the expression of denitrification in ex situ experiments. Soil Biology and Biochemistry 57, 606–614.

Osborne, B.B., Bestelmeyer, B.T., Currier, C.M., Homyak, P.M., Throop, H.L., Young, K., Reed, S.C., 2022a. The consequences of climate change for dryland biogeochemistry. New Phytologist 236, 15–20.

Osborne, B.B., Roybal, C.M., Reibold, R., Collier, C.D., Geiger, E., Phillips, M.L., Weintraub, M.N., Reed, S.C., 2022b. Biogeochemical and ecosystem properties in three adjacent semiarid grasslands are resistant to nitrogen deposition but sensitive to edaphic variability. Journal of Ecology 110, 1615–1631.

Prosser, J.I., Hink, L., Gubry-Rangin, C., Nicol, G.W., 2019. Nitrous oxide production by ammonia oxidisers: physiological diversity, niche differentiation and potential mitigation strategies. Global Change Biology 26, 103–118.

Püspök, J.F., Zhao, S., Calma, A.D., Vourlitis, G.L., Allison, S.D., Aronson, E.L., Schimel, J.P., Hanan, E.J., Homyak, P.M., 2022. Effects of Experimental Nitrogen Deposition on Soil Organic Carbon Storage in Southern California Drylands, vol. 29, pp. 1660–1679.

R Core Team, 2023. R: A Language and Environment for Statistical Computing.

Ravishankara, A.R., Daniel, J.S., Portmann, R.W., 2009. Nitrous oxide ($N_2O$): the dominant ozone-depleting substance emitted in the 21st century. Science 326, 123–125.

Ren, J., Hanan, E., Greene, A.C., Tague, C., Krichels, A., Burk, W., Schimel, J., Homyak, P.M., 2024. Simulating the role of biogeochemical hotspots in driving nitrogen export from dryland watersheds. Water Resources Research. https://doi.org/10.1029/2023WR036008.

Rotthauwe, J.H., Witzel, K.P., Liesack, W., 1997. The ammonia monooxygenase structural gene amoA as a functional marker: molecular fine-scale analysis of natural ammonia-oxidizing populations. Applied and Environmental Microbiology 63, 4704–4712.

Scholes, M.C., Martin, R., Scholes, R.J., Parsons, D., Winstead, E., 1997. NO and $N_2O$ emissions from savanna soils following the first simulated rains of the season. Nutrient Cycling in Agroecosystems 48, 115–122.

Sexstone, A.J., Revsbech, N.P., Parkin, T.B., Tiedje, J.M., 1985. Direct measurement of oxygen profiles and denitrification rates in soil aggregates. Soil Science Society of America Journal 49, 645–651. Soil Science Society of America.

Sha, T., Ma, X., Zhang, H., Janechek, N., Wang, Yanyu, Wang, Yi, Castro García, L., Jenerette, G.D., Wang, J., 2021. Impacts of soil $NO_x$ emission on $O_3$ air quality in rural California. Environmental Science and Technology. https://doi.org/10.1021/acs.est.0c06834.

Sickman, J.O., James, A.E., Fenn, M.E., Bytnerowicz, A., Lucero, D.M., Homyak, P.M., 2019. Quantifying atmospheric N deposition in dryland ecosystems: a test of the Integrated Total Nitrogen Input (ITNI) method. The Science of the Total Environment 646, 1253–1264.

Slessarev, E.W., Greene, A.C., Homyak, P.M., Ying, S.C., Schimel, J.P., 2021. High resolution measurements reveal abiotic and biotic mechanisms of elevated nitric oxide emission after wetting dry soil. Soil Biology and Biochemistry 160, 108316.

Smith, M.S., Firestone, M.K., Tiedje, J.M., 1978. The acetylene inhibition method for short-term measurement of soil denitrification and its evaluation using Nitrogen-13. Soil Science Society of America Journal 42, 611–615.

Soil Survey Staff, Natural Resources conservation Service, United States department of agriculture, 2019. Official soil series descriptions [WWW Document]. Web Soil Survey. URL. https://websoilsurvey.nrcs.usda.gov/app/, 1.10.24.

Song, T., Zhang, X., Li, J., Wu, X., Feng, H., Dong, W., 2021. A review of research progress of heterotrophic nitrification and aerobic denitrification microorganisms (HNADMs). The Science of the Total Environment 801, 149319.

Taylor, A.E., Vajrala, N., Giguere, A.T., Gitelman, A.I., Arp, D.J., Myrold, D.D., Sayavedra-Soto, L., Bottomley, P.J., 2013. Use of aliphatic n-alkynes to discriminate soil nitrification activities of ammonia-oxidizing thaumarchaea and bacteria. Applied and Environmental Microbiology 79, 6544–6551.

Thion, C., Prosser, J.I., 2014. Differential response of nonadapted ammonia-oxidising archaea and bacteria to drying-rewetting stress. FEMS Microbiology Ecology 90, 380–389.

Tian, H., Xu, R., Canadell, J.G., Thompson, R.L., Winiwarter, W., Suntharalingam, P., Davidson, E.A., Ciais, P., Jackson, R.B., Janssens-Maenhout, G., Prather, M.J., Regnier, P., Pan, N., Pan, S., Peters, G.P., Shi, H., Tubiello, F.N., Zaehle, S., Zhou, F., Arneth, A., Battaglia, G., Berthet, S., Bopp, L., Bouwman, A.F., Buitenhuis, E.T., Chang, J., Chipperfield, M.P., Dangal, S.R.S., Dlugokencky, E., Elkins, J.W., Eyre, B. D., Fu, B., Hall, B., Ito, A., Joos, F., Krummel, P.B., Landolfi, A., Laruelle, G.G., Lauerwald, R., Li, W., Lienert, S., Maavara, T., MacLeod, M., Millet, D.B., Olin, S., Patra, P.K., Prinn, R.G., Raymond, P.A., Ruiz, D.J., van der Werf, G.R., Vuichard, N., Wang, J., Weiss, R.F., Wells, K.C., Wilson, C., Yang, J., Yao, Y., 2020.

A comprehensive quantification of global nitrous oxide sources and sinks. Nature 586, 248–256.

Yahdjian, L., Gherardi, L., Sala, O.E., 2011. Nitrogen limitation in arid-subhumid ecosystems: a meta-analysis of fertilization studies. Journal of Arid Environments. https://doi.org/10.1016/j.jaridenv.2011.03.003.

Zhu-Barker, X., Cavazos, A.R., Ostrom, N.E., Horwath, W.R., Glass, J.B., 2015. The importance of abiotic reactions for nitrous oxide production. Biogeochemistry 126, 251–267.